

## SELF-DRIVING CHARACTERISTICS OF A PUMPLESS WATER ELECTROLYZER USING WATER-BASED FERROFLUID

*R. Somiya*<sup>1\*</sup>, *Y. Iwamoto*<sup>1</sup>, *Y. Ido*<sup>1</sup>, *A. Mitani*<sup>2</sup>

<sup>1</sup> *Nagoya Institute of Technology, Gokiso-cho, Showa-ku, Nagoya, Aichi, 466-8555, Japan*

<sup>2</sup> *Sumitomo Electric Industries, Ltd., 1-1-1 Koyakita, Itami, Hyogo, 664-0016, Japan*

\**e-Mail: r.somiya.199@stn.nitech.ac.jp*

The implementation of water electrolysis from lunar water sources facilitates the direct generation of hydrogen for rocket fuel and oxygen, which is essential for sustaining human life in space. Given the considerable costs associated with launching equipment into space, water electrolysis devices that operate in this environment must be smaller and lighter in order to be economically viable. This study proposes a pumpless water electrolysis device utilizing water-based ferrofluid. When non-magnetic hydrogen and oxygen bubbles are generated in a water-based magnetic fluid during water electrolysis under a non-uniform magnetic field, the balance of magnetic body force is disrupted, causing a driving force to act on the fluid. In this study, the driving force was experimentally verified using the PEM-type water electrolysis method. The findings have revealed that the proposed system can effectively function as a pump in removing the generated bubbles and self-supply water to the electrode.

### **Introduction.**

The Artemis Program, devised in the United States in 2017, is an initiative with the objective of facilitating lunar exploration and the construction of lunar bases. This initiative has prompted governments and numerous private companies across the globe to engage in lunar development initiatives, thereby extending both human habitation and economic activity to the Moon. One rationale for this is the potential abundance of water resources on the Moon [1,2]. The feasibility of water electrolysis using lunar water resources would allow for the production of hydrogen which can be used as rocket fuel, and oxygen which is essential for human life activities on the Moon. Using the Moon, where the gravitational pull is approximately one-sixth that of Earth, as a refueling base for spacecraft would render space exploration to Mars and asteroids more cost-effective than refueling on Earth [3].

The cost of transporting materials from Earth to the Moon is typically estimated at approximately 1 million dollars per kilogram. It is, therefore, essential that water electrolysis devices operating on the Moon are both lightweight and compact. Furthermore, in microgravity environments, such as space, buoyancy from gravitational forces is significantly reduced, which can hinder bubble detachment from electrodes and potentially lower electrolysis efficiency [4, 5]. To address this challenge, a methodology has been proposed wherein the application of magnetic fields induces magnetically driven buoyancy forces, facilitating the motion, separation, and collection of gas bubbles in microgravity conditions [6].

This study proposes the development of a pumpless water electrolysis device utilizing water-based ferrofluid. Fig. 1 provides a simplified schematic of the PEM-type water electrolysis system [7]. Traditional circulation systems incorporate numerous moving parts and components, making operations in spaces resource- and personnel-constrained environment complex, with additional maintenance challenges. In contrast, the proposed

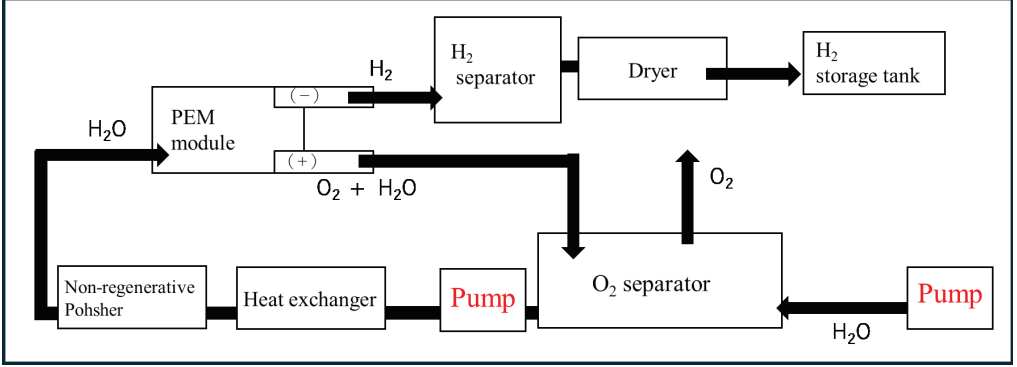


Fig. 1. Schematic diagram of the low-pressure type electrolyzer.

system eliminates conventional pumps and employs instead the magnetic properties of ferrofluid to facilitate water supply to the electrodes and bubble discharge aiming to simplify and miniaturize the system.

A water-based ferrofluid is defined as a fluid in which ferromagnetic nanoparticles with a diameter of approximately 10 nm are stably dispersed in water [8]. The potential of ferrofluids as functional materials has been the subject of considerable research, with the development of self-driving energy conversion systems utilizing gas-liquid two-phase flow representing a notable area of investigation [9, 10]. In this study, we evaluate the driving force performance of a system that employs the gas-liquid two-phase flow generated during water electrolysis using a water-based ferrofluid.

## 1. Experiment.

*1.1. Pumpless PEM water electrolysis device.* The operating principle of self-driven using gas-liquid two-phase flow in a non-uniform magnetic field of ferrofluid is illustrated in Fig. 2. The void fraction of bubbles in the ferrofluid results in a proportional decrease in the magnetization, with the magnetic body force expressed by the following equation:

$$\mathbf{F}_m = \mathbf{M} \cdot \nabla \mathbf{H} = \mu_0 \chi (1 - \alpha) \mathbf{H} \cdot \nabla \mathbf{H}, \quad (1)$$

where  $\mathbf{F}_m$  is the magnetic body force,  $\mathbf{M}$  is the magnetization, and  $\mathbf{H}$  is the magnetic field,  $\mu_0$  is the permeability, and  $\chi$  is the magnetic susceptibility,  $\alpha$  is the void fraction. For  $x < 0$ , consider the upstream region, where there is a single-phase flow of magnetic fluid. For  $x > 0$ , the downstream region consists of a two-phase flow of magnetic fluid mixed with bubbles. When a non-uniform magnetic field gradient is applied, as illustrated in Fig. 2, a magnetic body force is generated in each region according to Eq. (1). This difference in magnetic body force due to the gas-bubble generation between the upstream and downstream regions creates a driving force in the positive  $x$ -axis direction.

Fig. 3 displays the schematic diagram of the PEM water electrolysis device fabricated in the present study. In a PEM water electrolysis process, water is supplied from the anode, hydrogen is produced at the cathode, and oxygen is discharged from the anode [11]. The chemical reactions occurring at the anode and cathode are represented as follows.

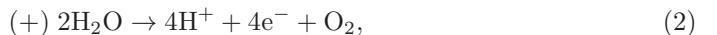
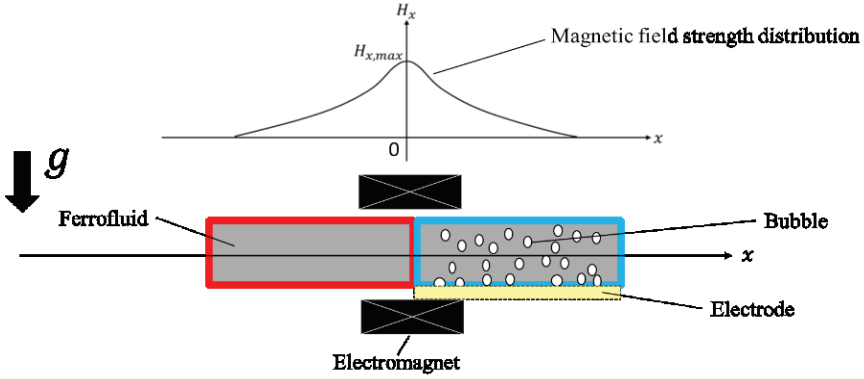
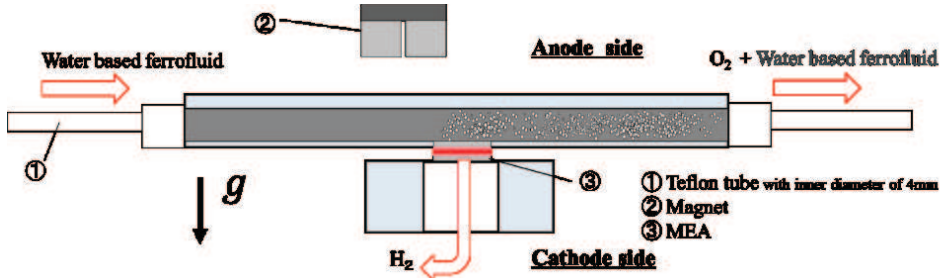


Fig. 4 illustrates the components of the custom-built PEM-type water electrolysis device used in this experiment. The main components of the PEM-type device employed

*Self-driving characteristics of a pumpless water electrolyzer using water-based ferrofluid*



*Fig. 2.* Operating principle of self-driven using gas-liquid two-phase flow in a non-uniform magnetic field of ferrofluid.



*Fig. 3.* Simplified diagram of a pumpless PEM water electrolysis device.

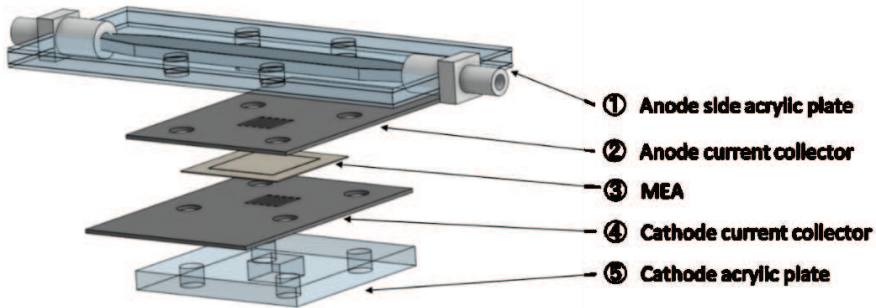


*Fig. 4.* Components of the electrolyzer.

in this study include an acrylic plate on the cathode side, two 1 mm thick stainless steel current collectors, a membrane electrode assembly (MEA), and an acrylic plate on the anode side to form the flow channel. These components are secured using screws and nuts, completing the assembly of the device. With the gravitational direction oriented downward, the upper section corresponds to the anode side and the lower section to the cathode side. The MEA consists of a Nafion polymer electrolyte membrane with electrode catalysts. Iridium serves as the catalyst on the anode side, while platinum is applied on the cathode side.



Table 1. Physical properties of Ferri1003S.

Density $\rho$ , [kg/m <sup>3</sup> ]	$1.39 \times 10^3$
Viscosity $\mu$ , [Pa·s]	more less $5 \times 10^{-2}$
Saturated magnetization $M_s$ , [mT]	20

Due to the equilibrium of atmospheric pressure, the fluid level in the inlet tank matches the fluid level at the end of the outlet Teflon tube. When electrolysis begins in the PEM device, a driving force acts, causing the fluid to overflow from the fluid level at the end of the outlet Teflon tube. The flowrate of the overflowing fluid is measured by the flow meter placed at the outlet side, which is used to evaluate the driving force.

In this experiment, the test fluid is a water-based ferrofluid, Ferri1003S (ICHINEN CHEMICALS Co., Ltd.), and a constant current of 30 mA is applied to the water electrolysis device using a potentiostat HZ 7000 (Hokuto Denko Corporation) for 400 seconds. Table 1 shows the physical properties of Ferri1003S.

The magnet, as shown in Fig. 7a, consists of two neodymium magnets and a yoke material. The magnetic field intensity distribution in the x-direction is as shown in Fig. 7b. As illustrated in Fig. 7c, the magnet is installed on the device, and the distance between the center axis of the magnet and the center axis of the bubble generation region is set to  $X$  mm. In this experiment, the driving force is evaluated under four conditions: without magnet, and with distances of  $X = 0, 2$ , and 4 mm.

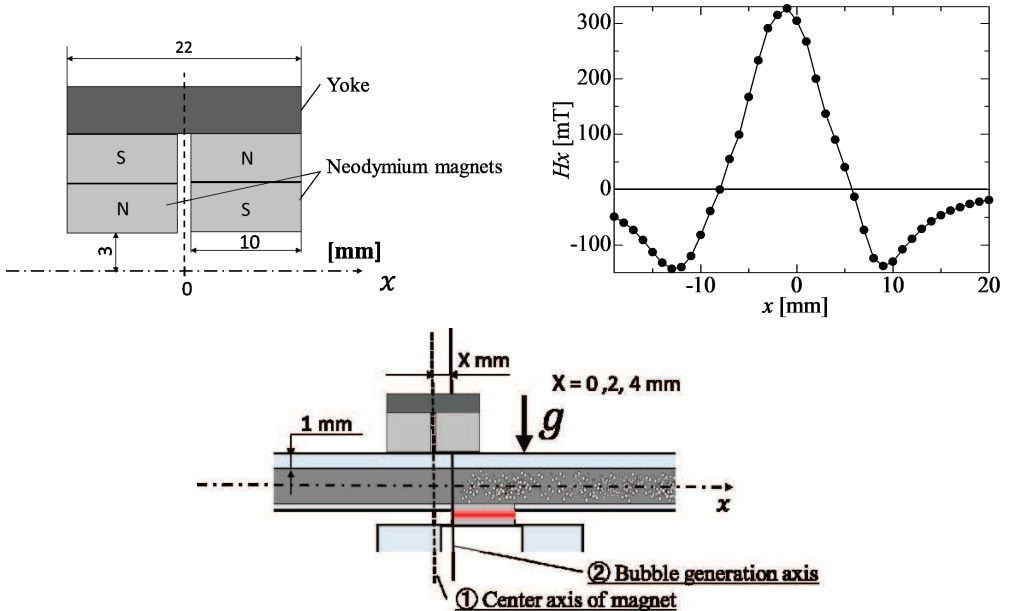


Fig. 7. (a) Structure of the magnet, (b) distribution of the magnetic field, (c) magnetic field conditions relative to the bubble generation region.

## 2. Results and discussion.

Fig. 8 shows a typical flowrate profile for each condition. In the absence of an applied magnetic field, the flowrate remained negligible and scarcely measurable; however, upon initiating water electrolysis with the application of a magnetic field, an immediate increase in flowrate was observed. This indicates that the proposed system is capable of effectively driving the ferrofluid through a magnetic body force, without the necessity for mechanical components such as pumps. It can be noted that the flowrate displays fluctuations due to the presence of bubbles. In this system, a bubble removal device has not been installed due to the risk of pressure loss in the self-driven mechanism. As a result, bubbles accumulate at the outlet of the flow channel and gradually merge. It is inferred that the vibrations generated during this merging process are reflected in fluctuations in the flowrate.

Fig. 9 presents a bar graph comparing the average flowrate under each condition. Three tests were conducted for each condition, and the graph includes the standard deviation. In the absence of the magnet, the flowrate was not observed. Under the magnetic field condition of  $X = 0$  mm, the average flowrate was  $95.9 \mu\text{l}/\text{min}$ ; for  $X = 2$  mm, the average flowrate was  $93.3 \mu\text{l}/\text{min}$ ; and for  $X = 4$  mm, the average flowrate was  $34.1 \mu\text{l}/\text{min}$ .

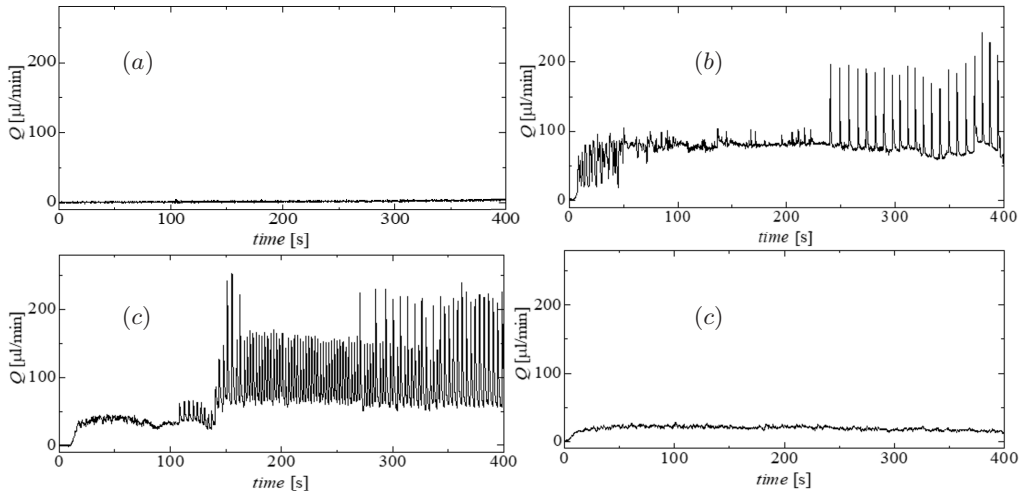


Fig. 8. Flowrate behavior at (a) non-magnet, (b)  $X = 0$  mm, (c)  $X = 2$  mm and (d)  $X = 4$  mm.

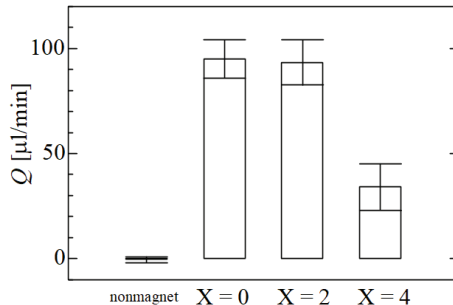


Fig. 9. Average flowrates with varying the distance  $X$ .

In the absence of the magnets, the flow rate was found to be negligible. However, under conditions with a magnetic field, it was confirmed that as the distance  $X$  between the magnet and the anode (the bubble generation region) increased, the magnetic field gradient acting on the bubble generation region decreased, resulting in a smaller flowrate. The mean flowrate under the magnetic field condition of  $X = 0$  mm was  $95.9 \mu\text{l}/\text{min}$ , with the total volume of flow over 400 seconds it was calculated to be  $6.4 \times 10^{-4}$  L. The theoretical volume of oxygen produced under the aforementioned conditions, with the effects of Faraday efficiency, intermolecular forces, and water pressure excluded, was  $6.9 \times 10^{-4}$  L. Upon comparing this value to the total flowrate, it was determined that the two are almost equivalent. It can, therefore, be concluded that, in this experiment, under the condition of  $X = 0$  mm, the most of the total flowrate measured by the flowmeter consists of the volume of oxygen bubbles. This result provides evidence that the control of oxygen bubble discharge on the outlet side was successful.

### **Conclusion.**

The objective of this study was to develop a pumpless water electrolysis system utilizing a water-based ferrofluid. The findings have revealed that the proposed system can effectively operate as a pump in removing the generated bubbles and self-supply the water to the electrode.

### **References**

- [1] S. LI, P. LUCEY *et al.* Direct evidence of surface exposed water ice in the lunar polar regions. *Proc. the National Academy of Sciences*, vol. 115 (2018), no. 36, pp. 8907–8912.
- [2] M. ANAND. Lunar Water: A brief review. *Earth, Moon, and Planets*, vol.107 (2010), pp. 65–73.
- [3] J. DAVENPORT, H. SCHUBERT *et al.* Space water electrolysis: space station through advanced missions. *Journal of Power Sources*, vol. 36 (1991), pp. 235–250.
- [4] A. GU, C. LI, J. XIE *et al.* Effects of micro convection on bubble displacement during water electrolysis under microgravity. *Journal of Emerging Investigators*, vol. 6 (2023).
- [5] Ö. AKAY, A. BASHKATOV *et al.* Electrolysis in reduced gravitational environments: current research perspectives and future applications. *NPJ Microgravity*, vol. 8 (2022).
- [6] A. ROMERO-CALVO, Ö. AKAY *et al.* Magnetic phase separation in microgravity. *NPJ Microgravity*, vol. 8 (2022).
- [7] L. ALLIDIÈRES, A. BRISSE *et al.* On the ability of PEM water electrolyzers to provide power grid services. *International Journal of Hydrogen Energy*, vol. 44 (2019), pp. 9690–9700.
- [8] C. SCHERER, AND A. FIGUEIREDO NETO. Ferrofluids: properties and applications. *Brazilian Journal of Physics*, vol. 35 (2005), no. 3A, pp. 718–727.
- [9] H. NISHIYAMA, S. KAMIYAMA *et al.* Basic study on an energy conversion system using gas-liquid two-phase flows of magnetic fluid. *JSME International Journal Series B*, vol. 39 (1996), no. 1, pp. 72–79.

- [10] Y. IWAMOTO, X. NIU *et al.* Magnetically-driven heat transport device using ferrofluid. *Journal of JSEM*, vol. 12 (2012), Special Issue, pp. s99–s104.
- [11] R. VINODH, T. PALANIVEL, S. KALANUR, AND G. POLLET. Recent advancements in catalyst coated membranes for water electrolysis: a critical review. *Energy Advances*, vol. 3 (2024), pp. 1144–1166.

Received 24.11.2024